



Compressibility Effects on Dielectric Barrier Discharge Actuation and Boundary Layer Receptivity

Marie Denison, Luca Massa
University of Texas at Arlington, TX

Outline



- Introduction
- Linear Stability Analysis Framework
- AMR Coupled Plasma-Navier and Stokes Solver
- Discharge Features
- Receptivity Analysis and Design Implications
- Summary

Outline



- Introduction
- Linear Stability Analysis Framework
- AMR Coupled Plasma-Navier and Stokes Solver
- Discharge Features
- Receptivity Analysis and Design Implications
- Summary



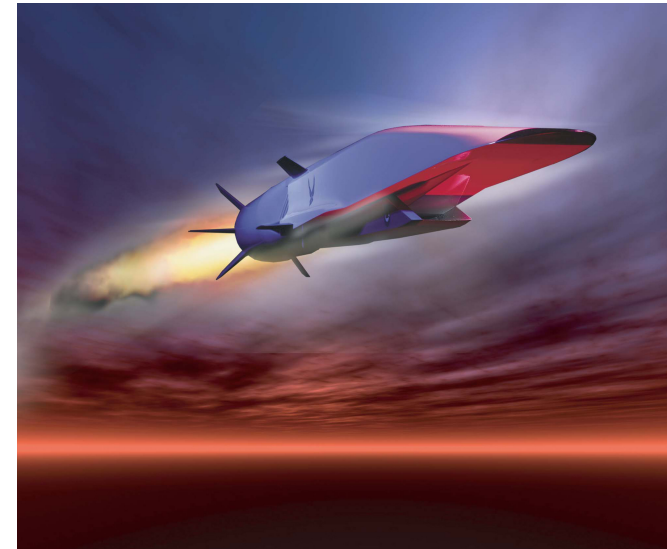
Motivation

Supersonic flow boundary layer instabilities

- Cross-flow dominated laminar-turbulent transition along supersonic cones and swept wings
- Turbulence and detachment in scramjet inlets, upstream shock propagation, unstart

Synthetic plasma roughness

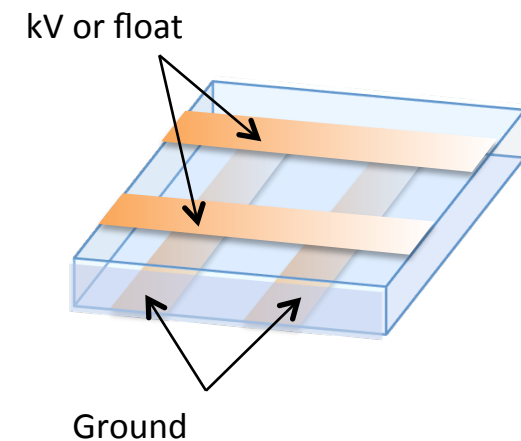
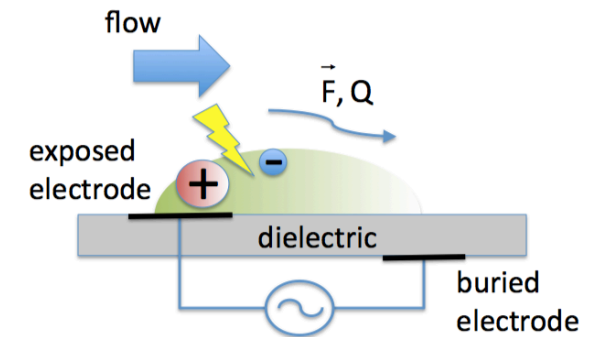
- Control of distributed Dielectric Barrier Discharge electrodes adapted to flight conditions
- For example subcritical forcing of stationary waves or boundary layer energization / thinning



Figures of Merit of DBD actuation



FOM	DBD	Solid Roughness
Control	yes: height, thrust, activation pattern, switch-off	no
BL penetration	volume forcing, horizontal/vertical jets	low
Wall thermal conductivity	low (<1.5W/Km)	depends
Power	electric supply, temporary drag	Drag
Weight	larger (mat. density, electrodes, wiring, supply, control)	lower
Reliability	dielectric breakdown, temperature limit, electrode wear-off	surface wear-off
Manufacturing effort and cost	larger	lower
TRL	low	high



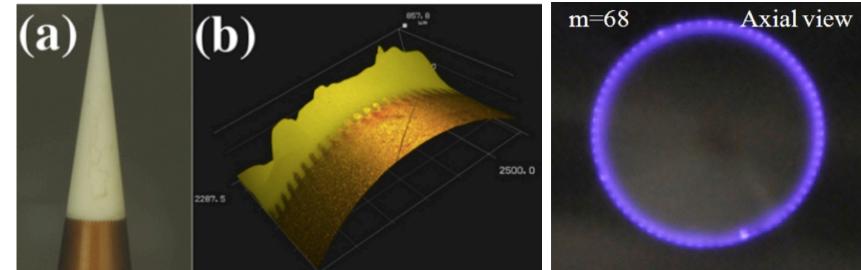
Challenges



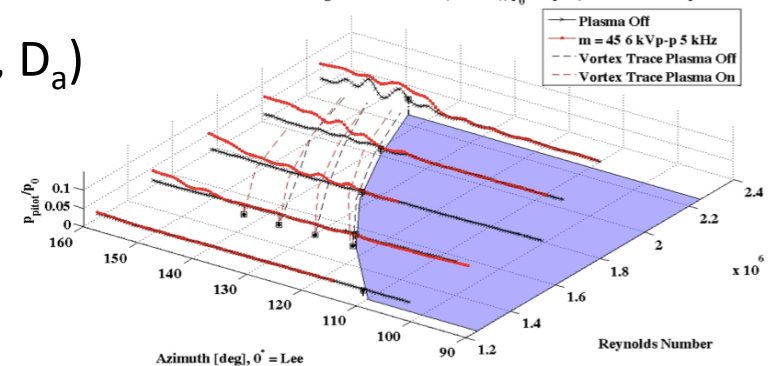
Y.C. Schuele, Ph.D., Univ. of Notre Dame, 2011

Physics:

- DBD atmospheric gas chemistry
- Heating, real gas effects
- Surface reactions
- Plasma-Flow energy coupling (T_e , T_g , n_{th} , D_a)



Azimuthal Scans at Constant Height Above Surface (0.04mm), $p_0=25$ psia, $m=68$ Plasma Tip



CFD and Receptivity Analysis:

- "Pulsing roughness"
- 3D Micro-filamentation
- Statistical characteristics, relation to surface properties
- Length ($\sim \mu\text{m}$ cathode sheath) and time scales (ps...s) \rightarrow model reduction
- HPC, automated refinement around discharges
- Experimental validation of gas models (flow on/off)

This Work



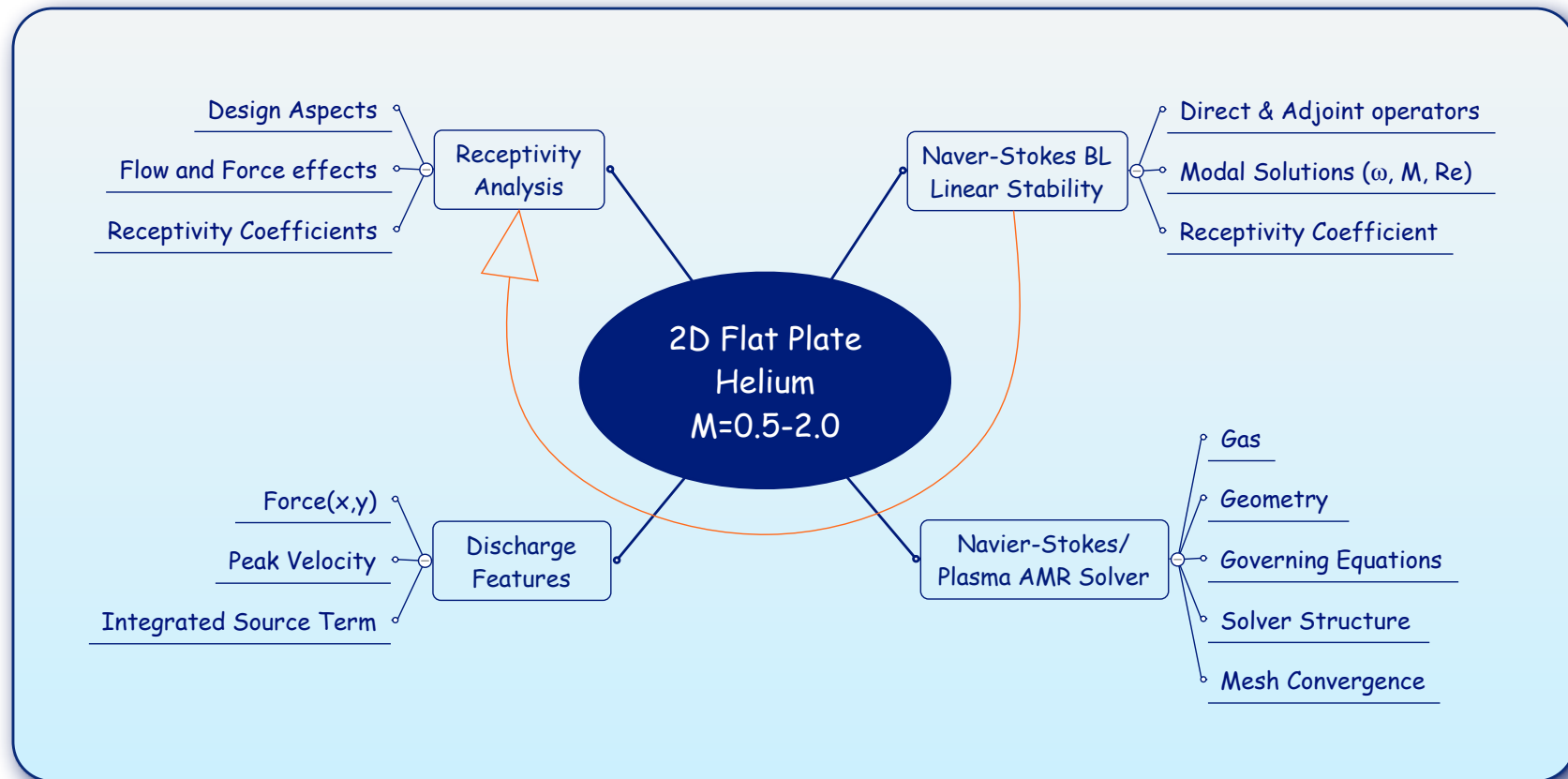
System

- 2D Flat plate
- 3-species Helium gas
- Eigenmode growth (Tollmien-Schlichting)

Research

- Study of compressibility effects
 - on DBD discharge features
 - on linear receptivity to DBD perturbation
- New coupled AMR Plasma Navier-Stokes solver (1-3D)
- Adjoint based formulation of the compressible boundary layer receptivity problem

This Work



Outline



- Introduction
- **Linear Stability Analysis Framework**
- AMR Coupled Plasma-Navier and Stokes Solver
- Discharge Features
- Receptivity Analysis and Design Implications
- Summary



Linear Stability Framework

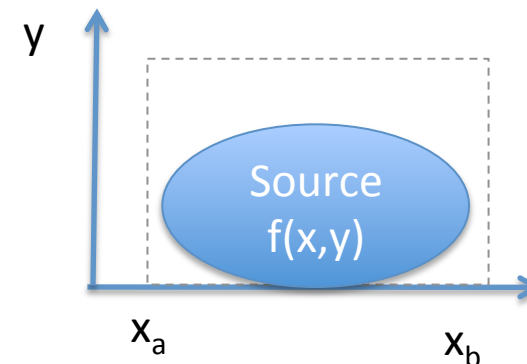
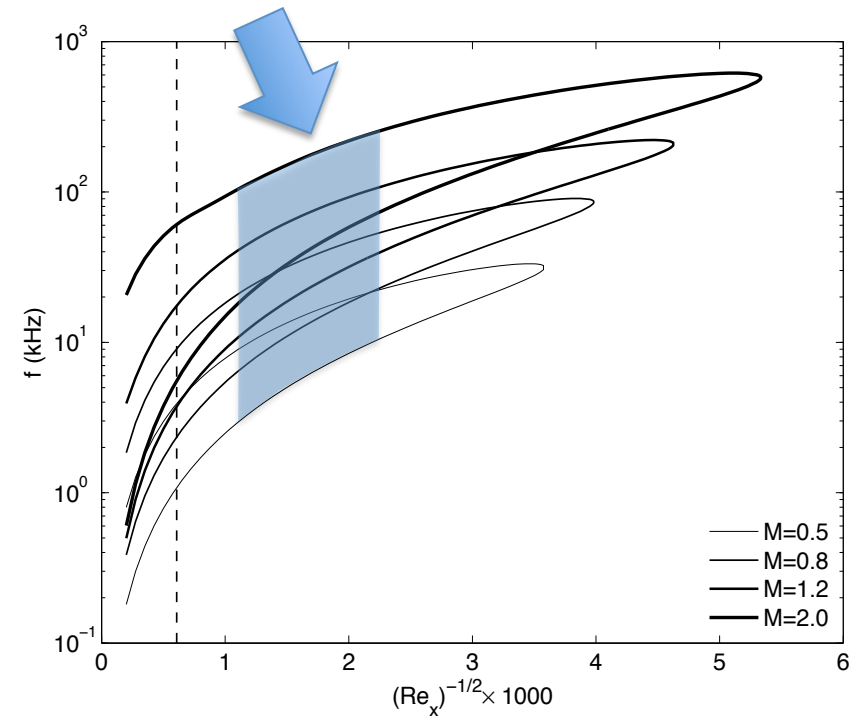
- DBD induced velocity $\sim \text{m/s} \ll u_\infty$
- Quasi-parallel approximation
- $\{M, \text{Re}\}$ range to support TS waves
- Non-dimensionalization, a.o.

$$L^* = \frac{x}{\text{Re}_x}, \text{Re}_x = \frac{\rho u_\infty^* x}{\mu_\infty^*}, \omega = \omega^* \frac{L^*}{u_\infty^*}$$

- Horizontal velocity perturbation from $f(x,y)\exp(-i\omega t)$ source term and discrete modes $u = \sum_k A_k \phi_k(y) e^{-i(\omega_k t - \alpha_k x)}$

where A_k is the receptivity coefficient

$$A_k = \frac{\int_a^b dx \int_0^\infty f(x,y) \hat{\phi}_k(y) e^{-i\alpha_k x} dy}{[\phi_k, \hat{\phi}_k]}$$





Adjoint Eigenproblem

- $\hat{\phi}_k$ in A_k is the adjoint mode to ϕ_k , obtained from the solution of the adjoint system itself derived from the *Euler-Lagrange's* identity

$$\phi \cdot \left(\Lambda \frac{\partial \hat{\phi}}{\partial t} + \hat{L}(\hat{\phi}) \right) + \hat{\phi} \cdot f = \frac{\partial \Gamma(\phi, \hat{\phi})}{\partial t} + \nabla \cdot J(\phi, \hat{\phi})$$

- Interpretation:

- Assume point unit force $f(x,y)=\delta(x_0,y_0)$,
- Normalize ϕ_k by $\max |\phi_k(y)|$ and $\hat{\phi}_k$ by $[\phi_k, \hat{\phi}_k] = 1$

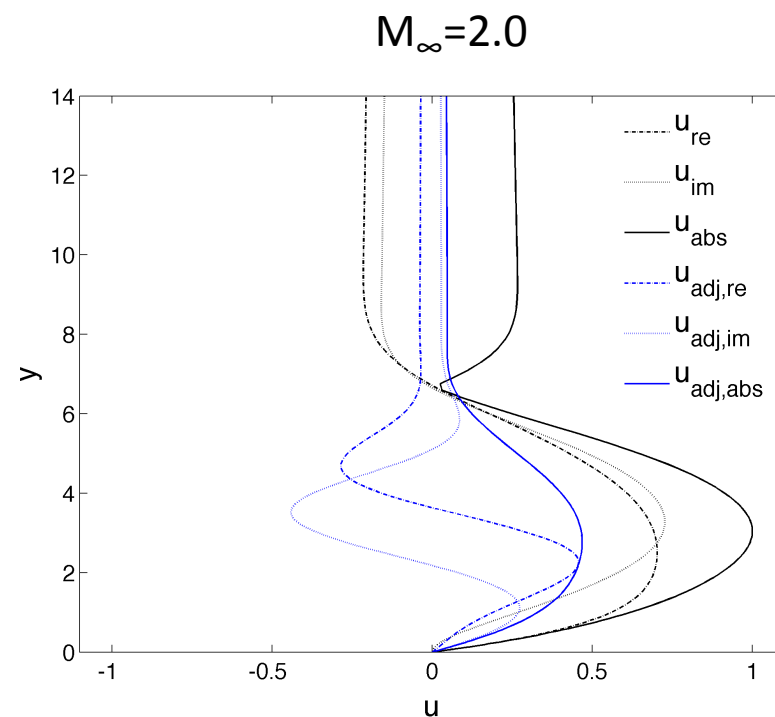
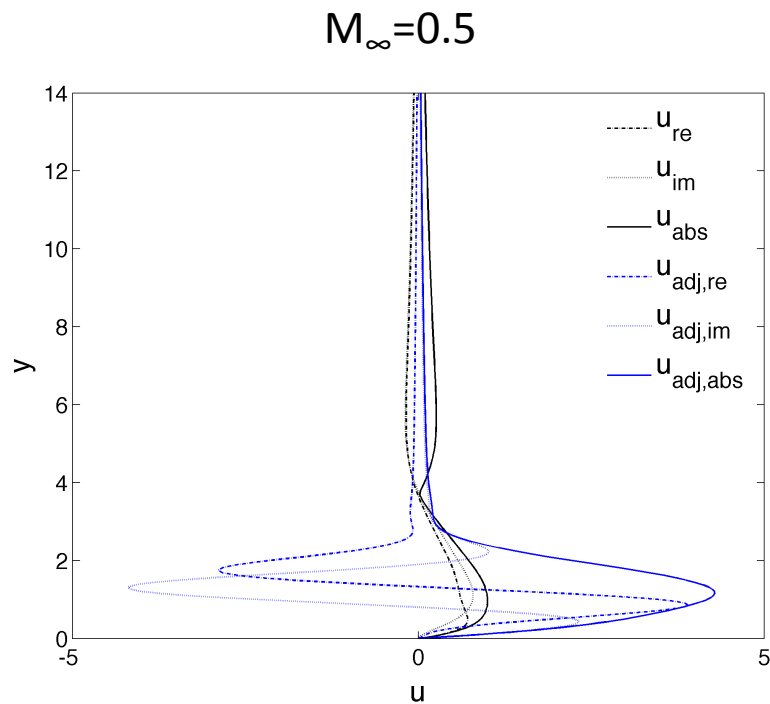
$$|A_k| = \hat{\phi}_k(y_0)$$

- The adjoint mode propagation velocity is opposite to the regular mode
➔ for $\text{Re}(\alpha) > 0$, mode amplification is upstream towards the source
- *The method allows testing multiple sources using the solutions of the homogeneous regular and adjoint eigenvalue problems*

Regular and Adjoint Mode Solutions



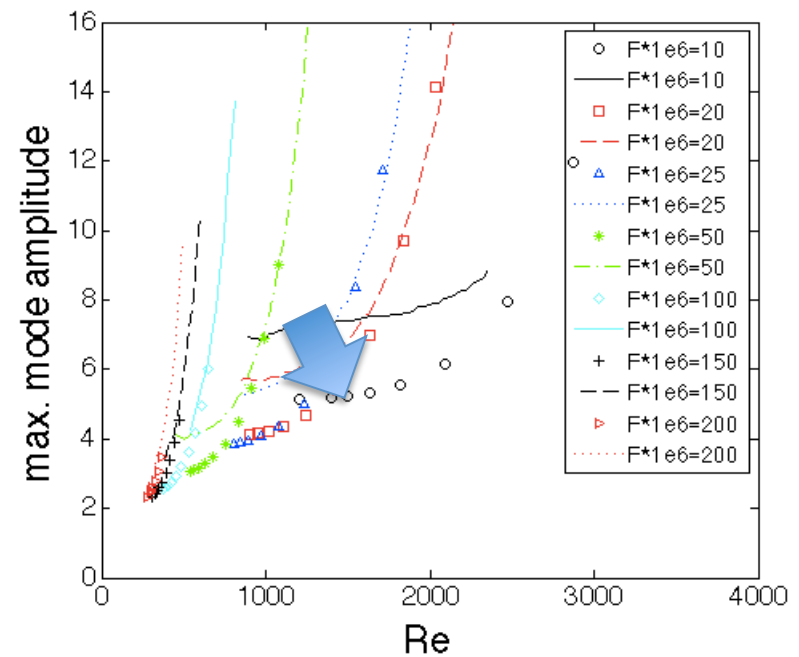
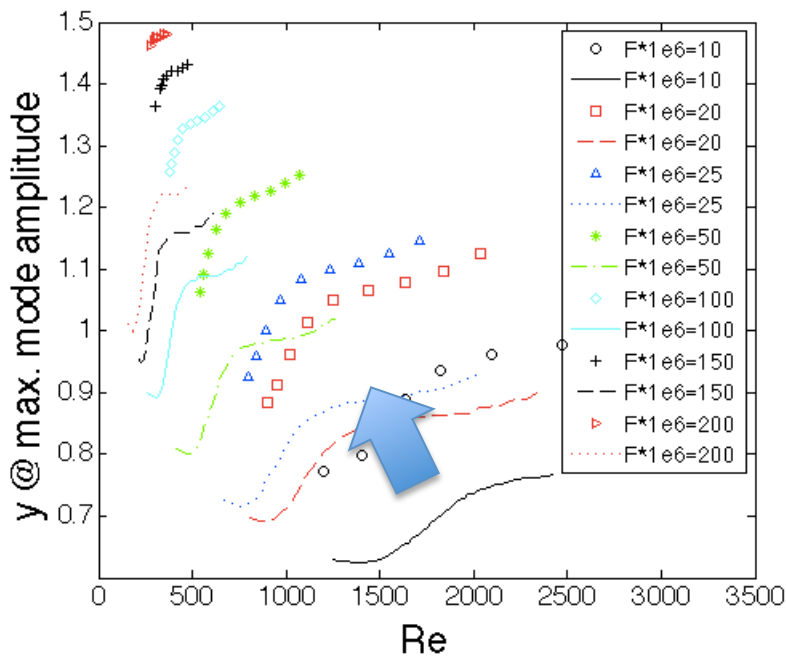
- Chebyshev τ -QZ method used to solve the eigenproblems
- At high M_∞ , the adjoint mode (unit-point-force sensitivity) decreases and the depth of its maximum increases





Comparison to incompressible case

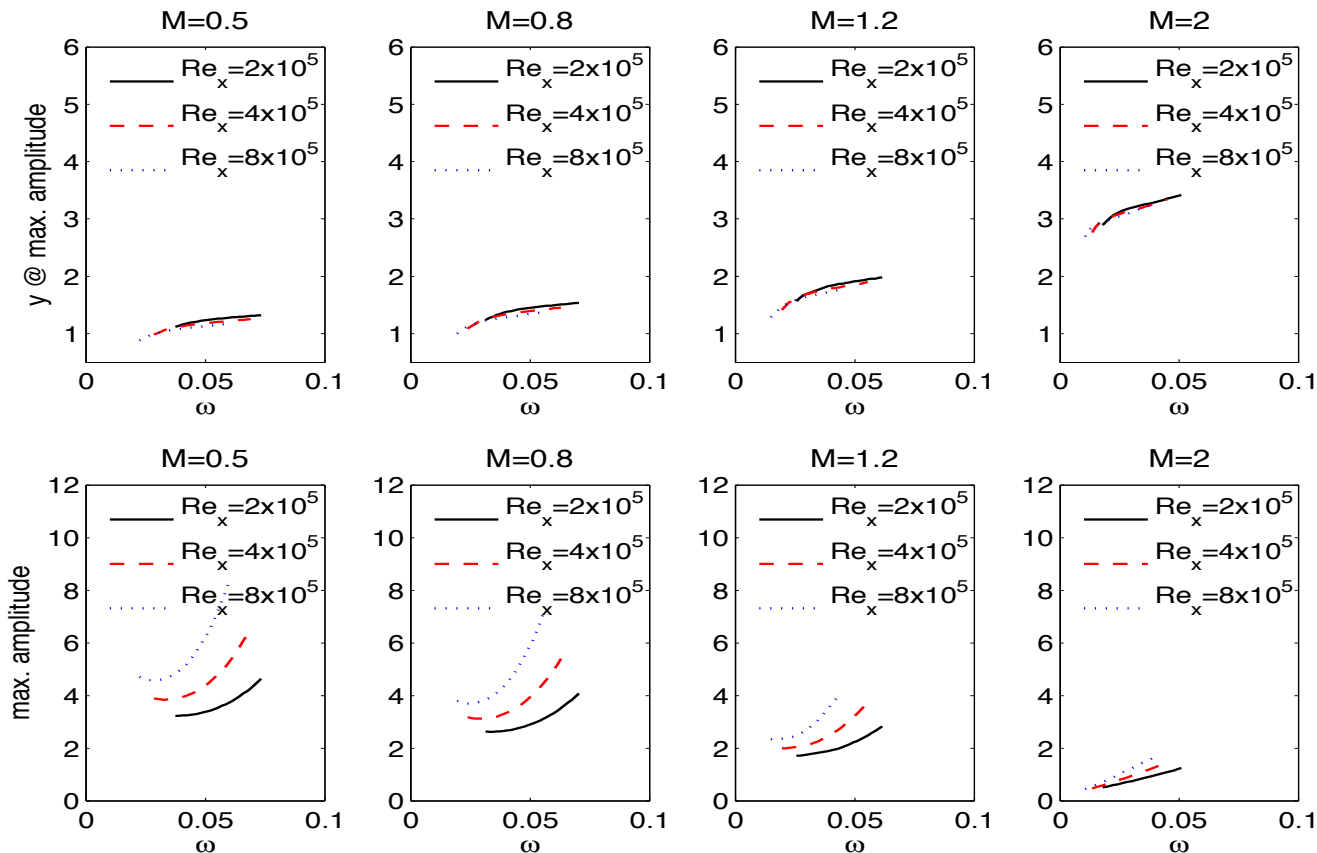
- D.C. Hill's results (J. Fluid Mech. '95) data well reproduced @ $M_\infty=0.1$ (lines)
- At $M_\infty=0.8$ (symbols), the mode depth increases and its amplitude decreases
 $F = \omega / \nu(\text{Re}_x)$



Adjoint modes



- Up to 3x depth increase and 1/9x amplitude decrease over M_∞ range
- Receptivity benefit in matching the source and adjoint profiles



Outline

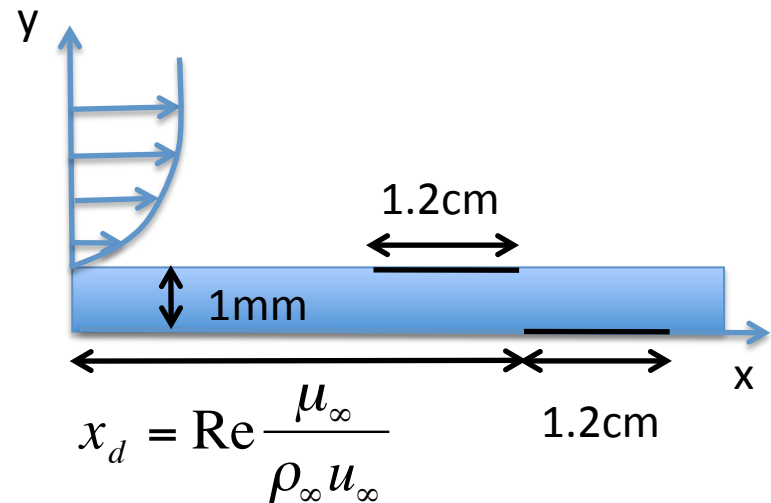


- Introduction
- Linear Stability Analysis Framework
- **AMR Coupled Plasma-Navier and Stokes Solver**
- Discharge Features
- Receptivity Analysis and Design Implications
- Summary

System and Regimes



- 2D Flat plate
 - 1mm dielectric thickness, 3.5 dielectric constant
 - 1.2cm electrode width
 - 2.45cm distance between downstream plate edge and electrode edge...
- Flow
 - $M_\infty = 0.5$ to 2.0
 - $Re = 2 \times 10^5$ to 8×10^5
 - Self-similar profile at inflow boundary
 - ... Momentum thickness for effective x_d
- Gas
 - Simplified helium chemistry (He, He+, e-)
 - Constant electron temperature (1eV)
 - impact ionization and recombination rates per *S. Roy, Phys. of Plasmas, Vol. 13, '06*
 - Reduced electric field dependent mobilities





AMR Solver

- Governing equations

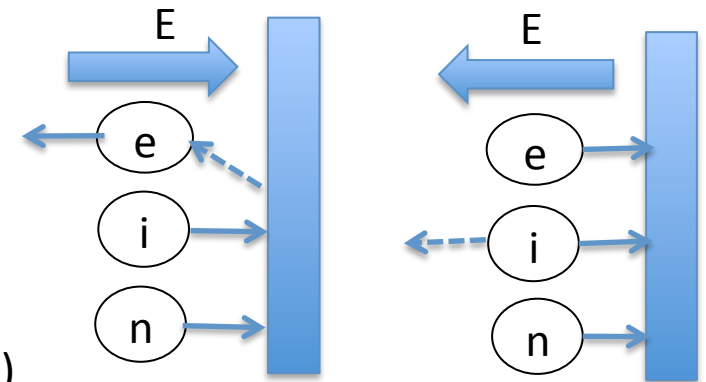
continuity:
$$\frac{\partial n_j}{\partial t} + \nabla \cdot \mathbf{F}_j = \sum_k G_{j,k}$$

drift-diffusion:
$$\mathbf{F}_j = n_j \mathbf{u}_j = \text{sign}(Z_j) n_j \mu_j \mathbf{E} - D_j \nabla n_j + n_j \mathbf{V}_j$$

Poisson:
$$\epsilon \nabla \cdot \mathbf{E} = \sum_j Z_j q_j n_j$$

- Wall boundary conditions

- 2,828V at the cathode, $f = 5\text{kHz}$
- adiabatic surface
- secondary emission at the cathode (coeff.=0.26)
- thermal flux and relevant charged species drift towards the wall
- gas/dielectric interface charge from the species flux towards the wall



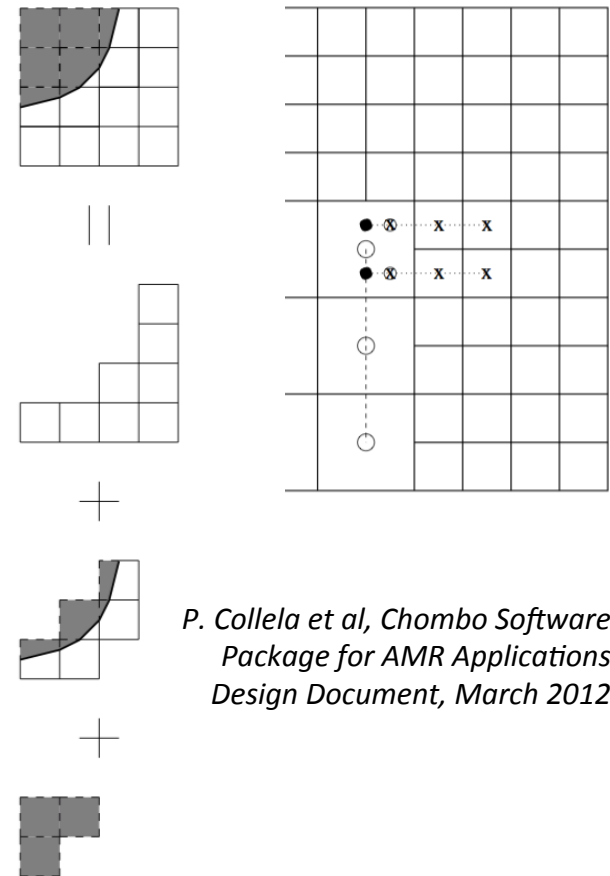
Dielectric displacement by stencil manipulation at the 1D embedded boundary

$$\frac{d\sigma_s}{dt} = \sum_j q Z_j \mathbf{F}_j \cdot \mathbf{n}, \quad (\epsilon_d \mathbf{E}_d - \epsilon_g \mathbf{E}_g) \cdot \mathbf{n} = \sigma_s$$

AMR Solver

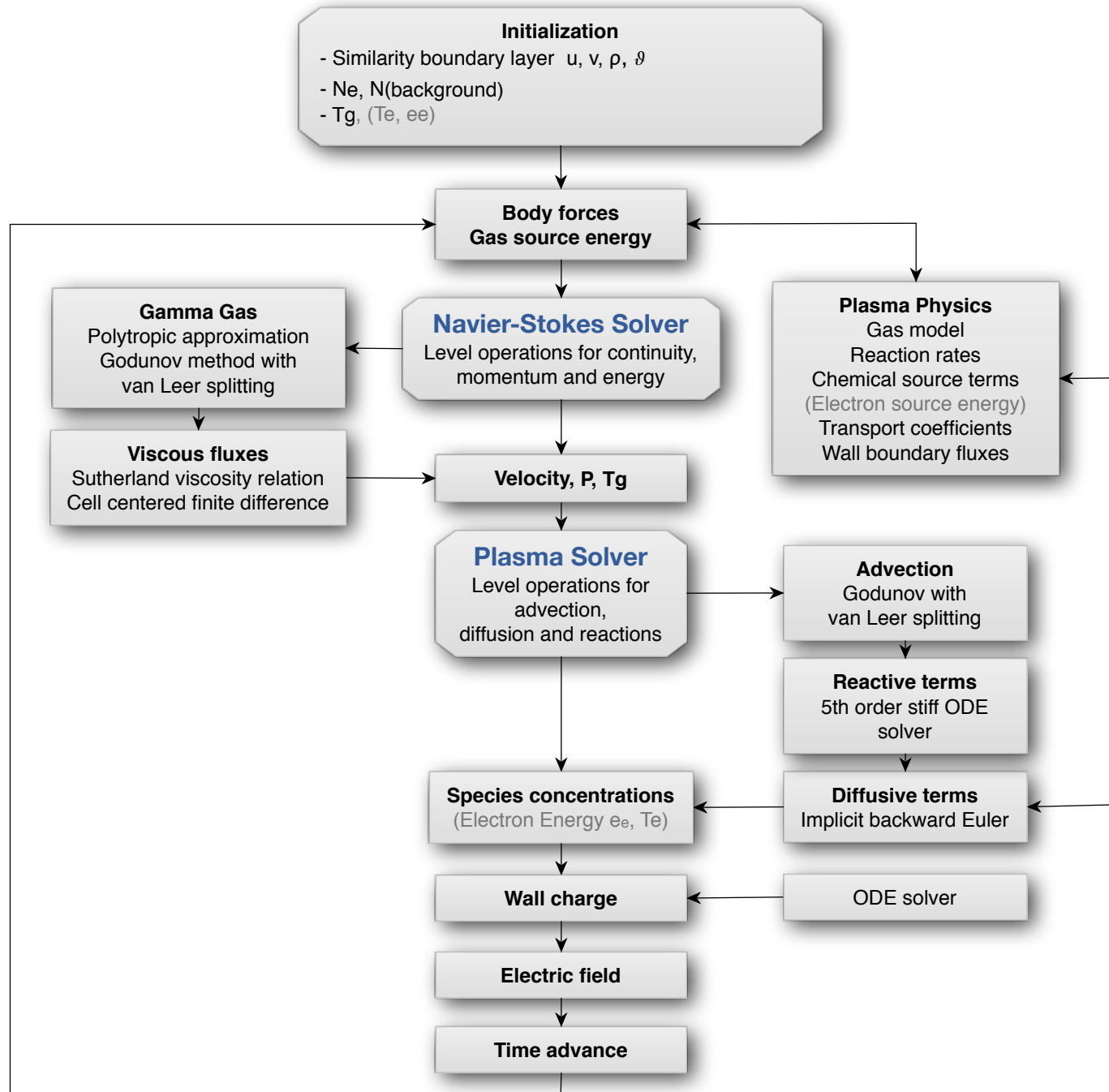


- Univ. of Berkeley's *Chombo* Adaptive Mesh Refinement C++ numerical framework for the solution of PDEs
 - block structured
 - embedded boundary
 - hierarchy of rectangular lattices communicating through ghost cells
 - graph representing the irregular cells
 - physics-based automated tagging and refinement
- Two independent meshes for flow and plasma, synchronized at coarse time steps
- Implemented on Texas Advanced Computing Center (TACC), Stampede HPC system



P. Collela et al, Chombo Software Package for AMR Applications Design Document, March 2012

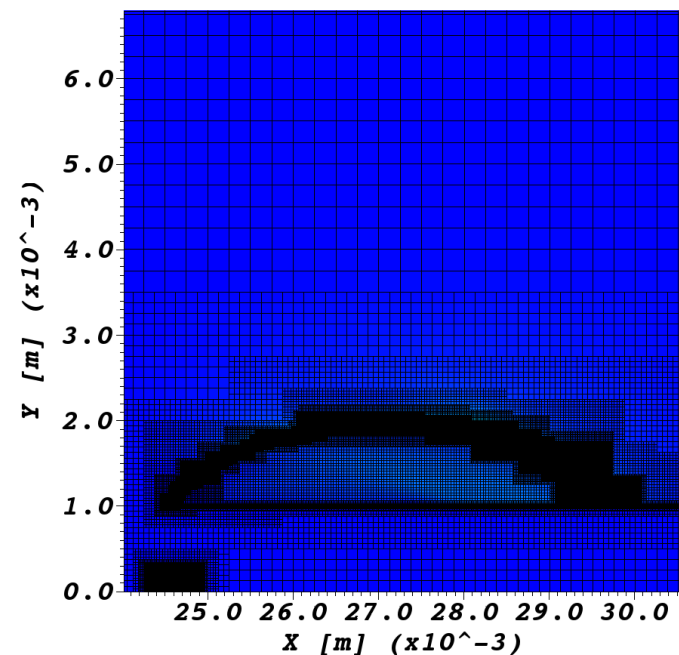
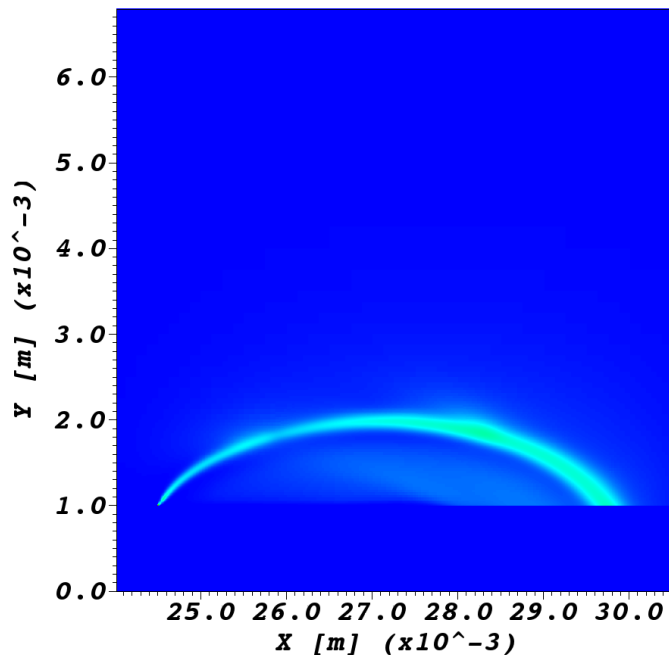
AMR solver





Adaptive Mesh Refinement

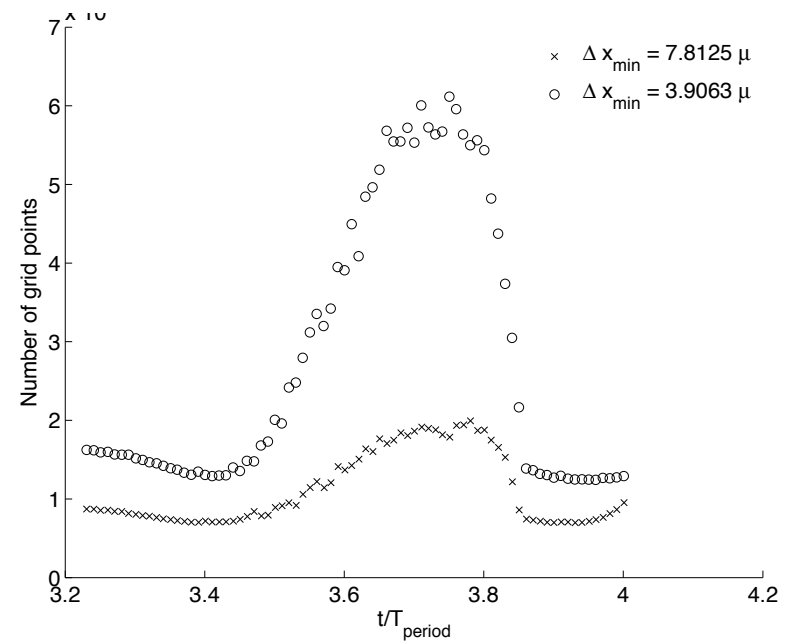
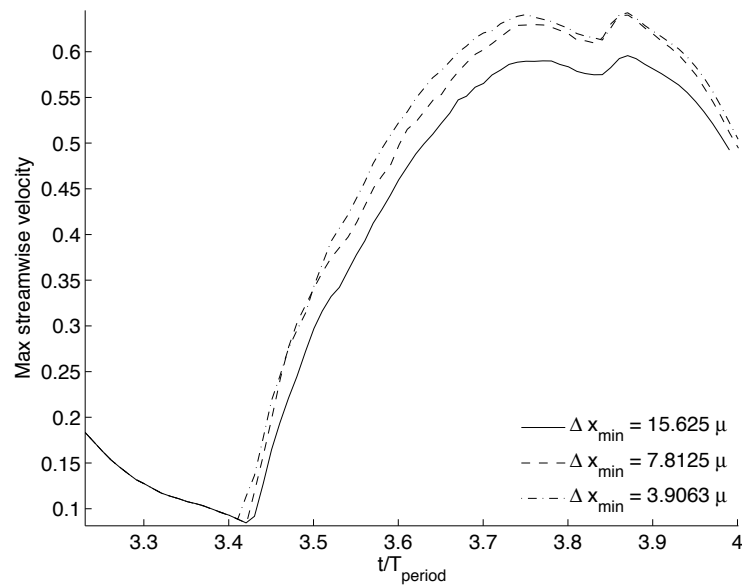
- $M_\infty=0.8$, $Re=0.8 \times 10^6$
- 7 refinement levels for the species
 - thresholds: $E > 2.5 \times 10^6$ V/m, $|F| > 250$ N/m³, $n_e = 1 \times 10^{-9}$ mol/m³
- 4 refinement levels for vorticity, threshold $|\omega|/u_\infty > 200$ m⁻¹
- CFL in the last periods = $CFL_a * (1 + M_\infty) \sim 0.28$





Convergence

- Periodic solution after 2-3 periods in studied M_∞ range
- Solution converged within 2-5% with 7 species levels
- Max. nr of grid points at $\sim 0.7 T$ ($@V_{\max}$), following the induced velocity



Outline

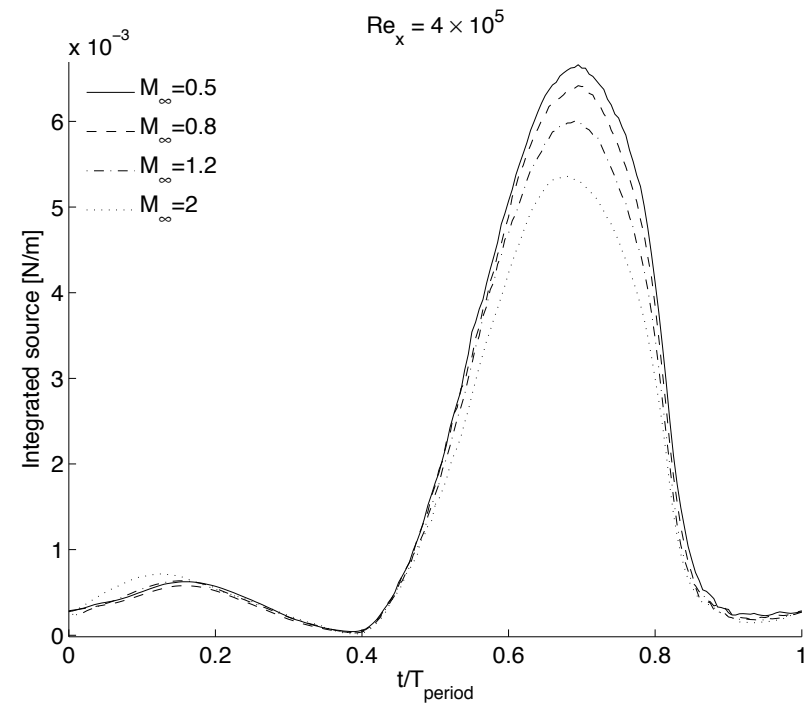
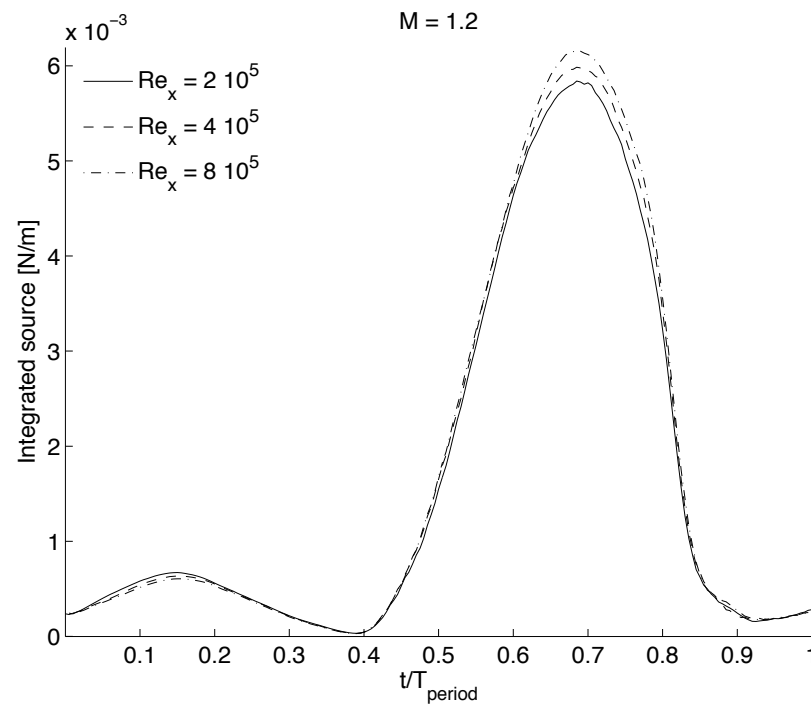


- Introduction
- Linear Stability Analysis Framework
- AMR Coupled Plasma-Navier and Stokes Solver
- **Discharge Features**
- Receptivity Analysis and Design Implications
- Summary



Integrated source term

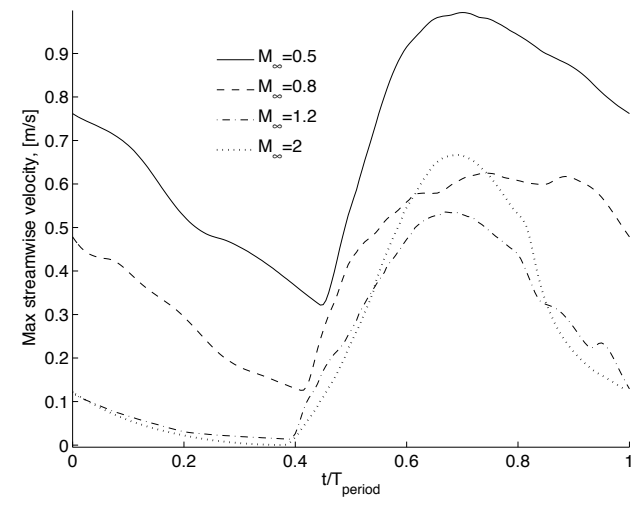
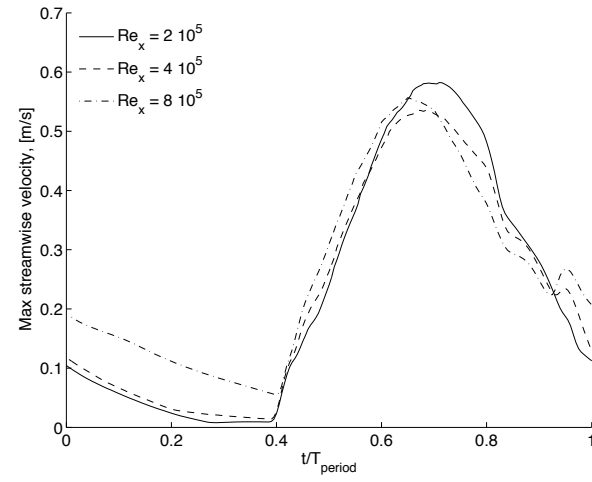
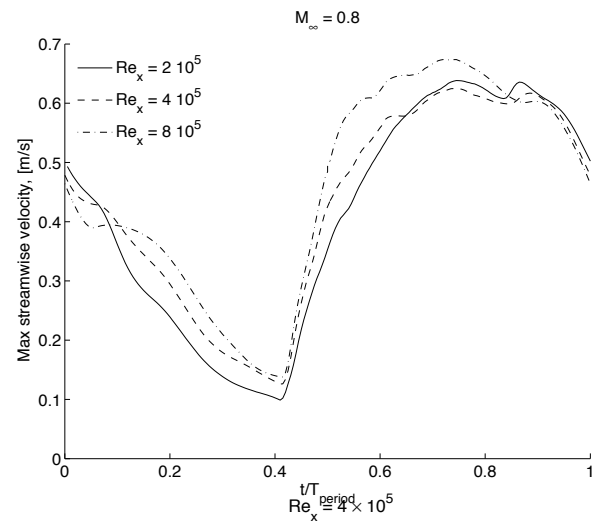
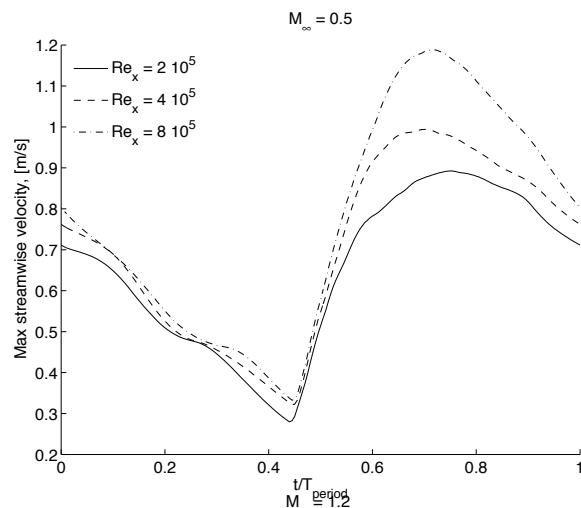
- Monotonic integrated source term $S_{\text{int}} \int_A \sqrt{f_x^2 + f_y^2} dA$ [N/m]
reduction with decreasing Reynolds nr and increasing M_∞



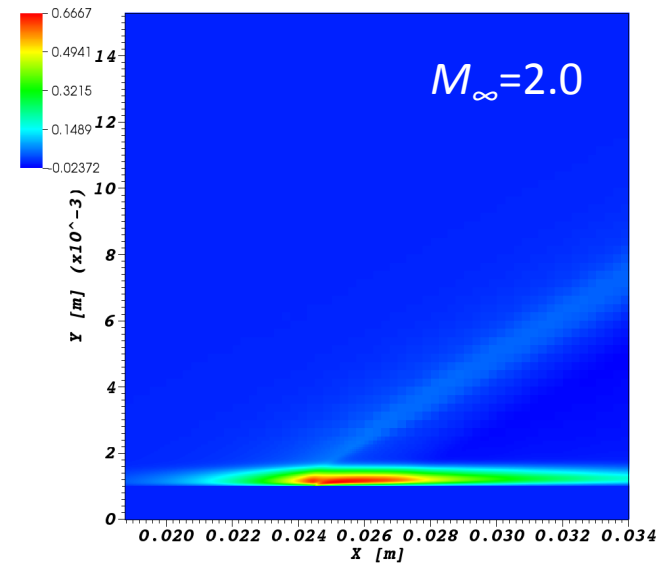
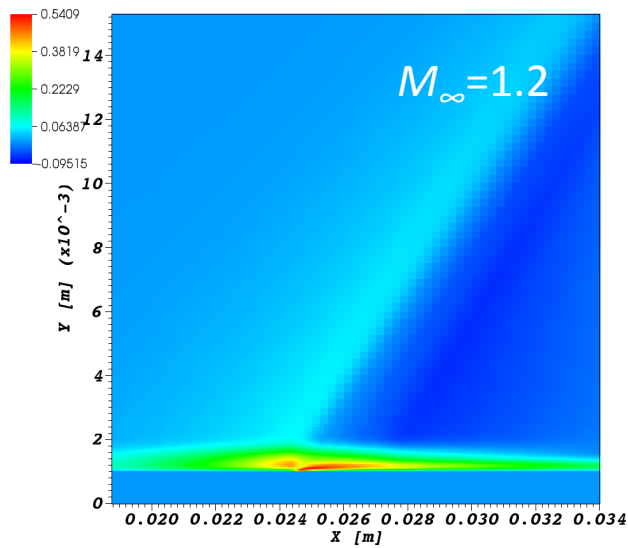
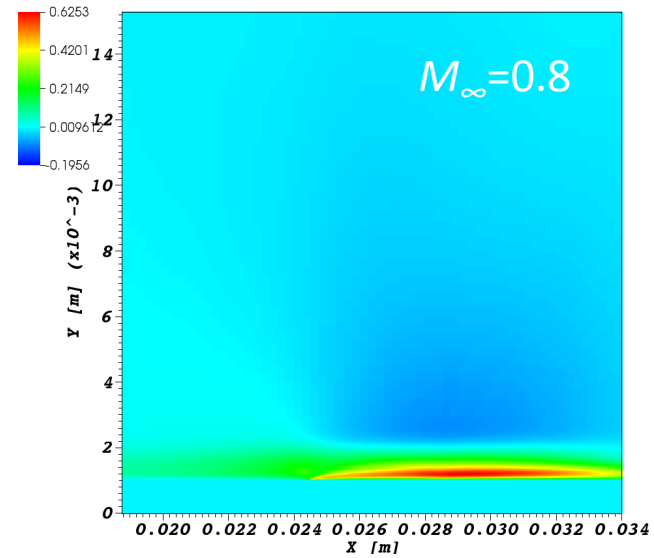
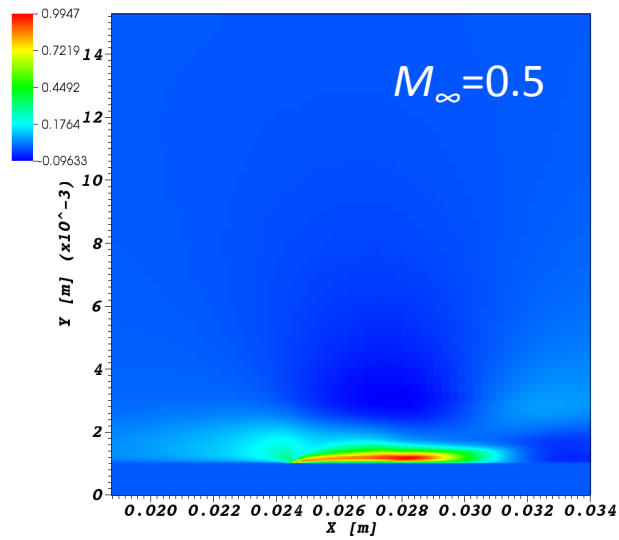


Peak velocity

- Non-monotonic Reynolds effect with increasing M_∞



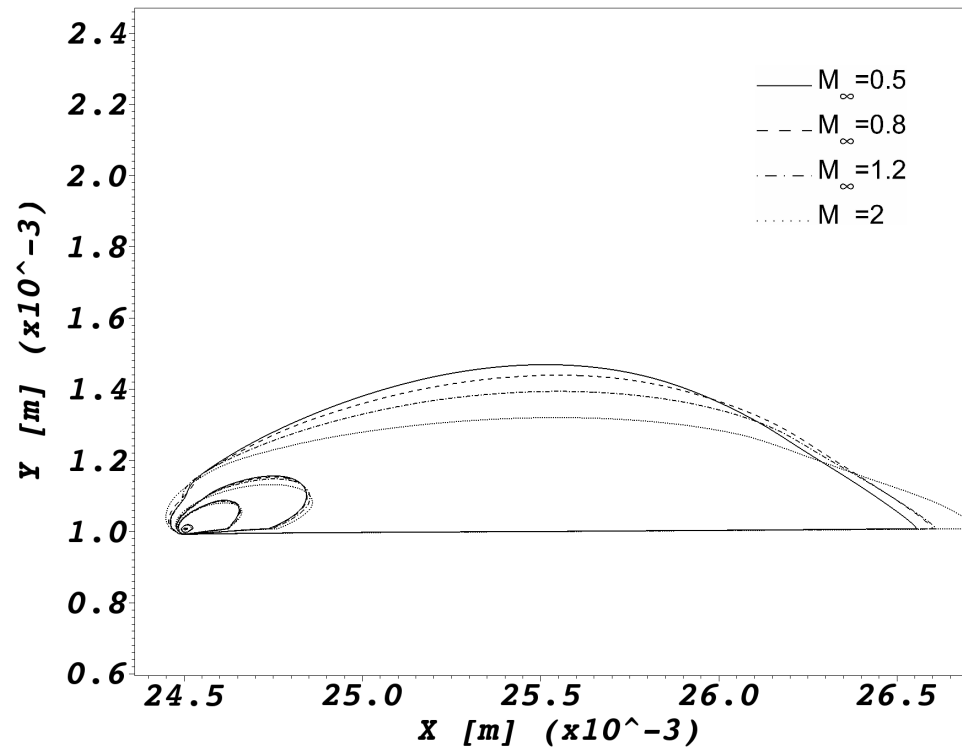
Velocity Profile





Force profile

- 5 contours at $S_x = \{1 \times 10^3, 5 \times 10^3, 1 \times 10^4, 5 \times 10^4, 1 \times 10^5\}$ N/m³
- Profile flattening/elongation with increasing M_∞



Outline

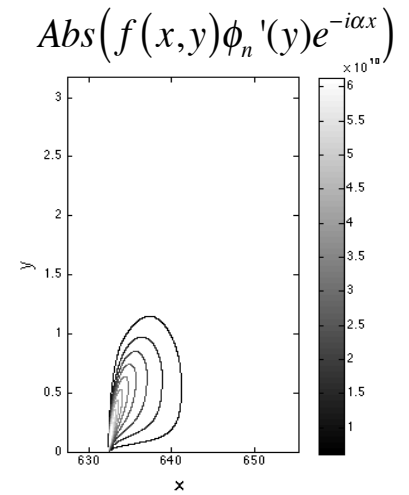
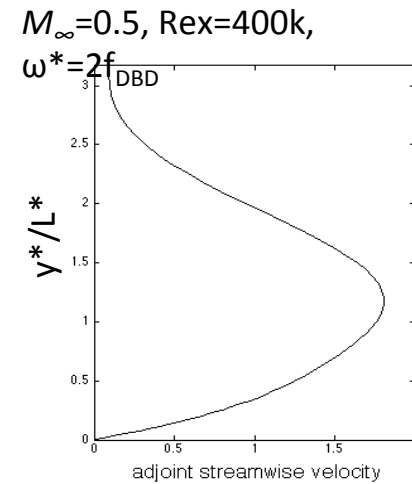
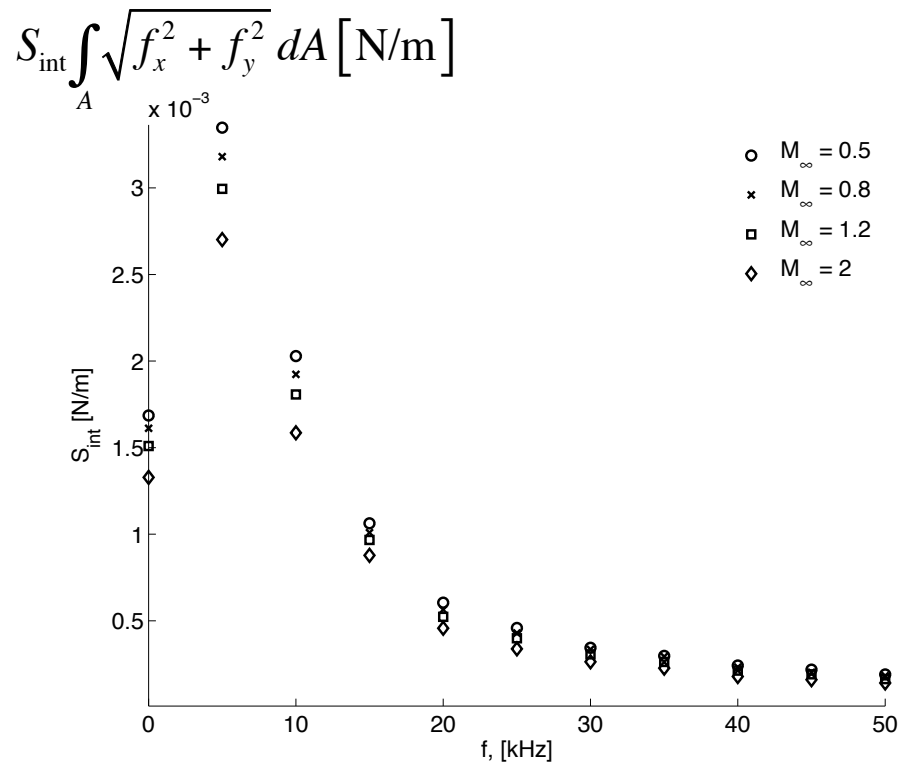


- Introduction
- Linear Stability Analysis Framework
- AMR Coupled Plasma-Navier and Stokes Solver
- Discharge Features
- **Receptivity Analysis and Design Implications**
- Summary

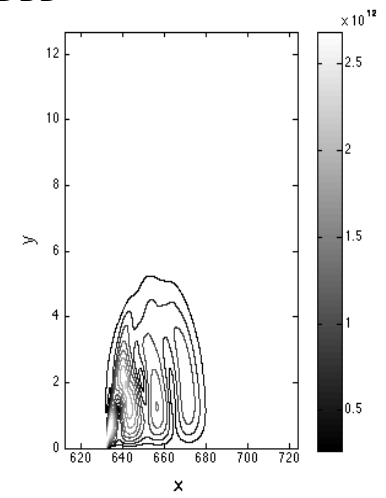
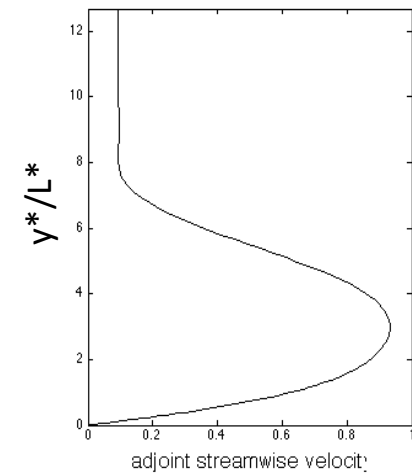


Force FFT Decomposition

- Model decomposition with FFTW
- 200 samples per actuation period
- steep amplitude decrease with f



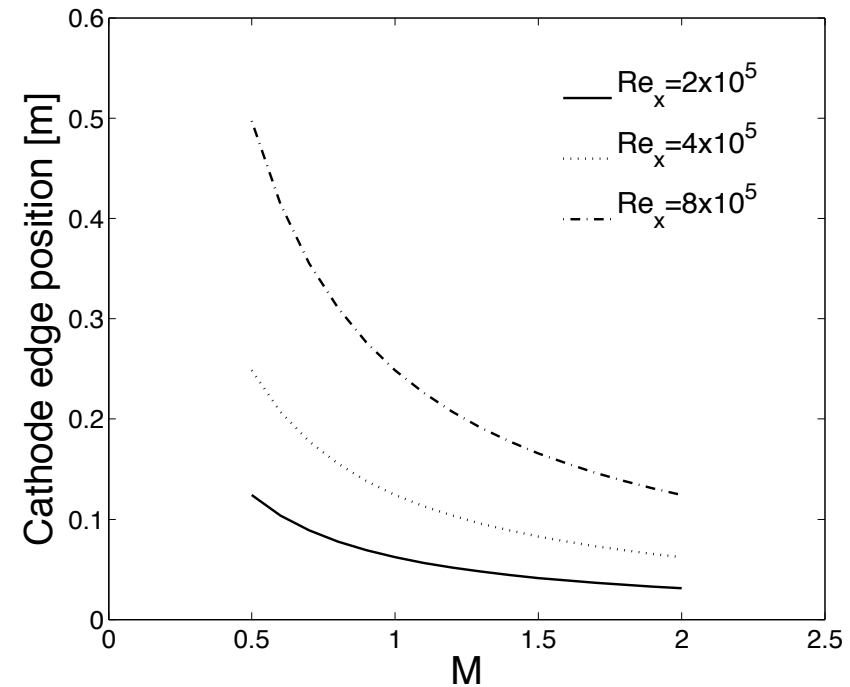
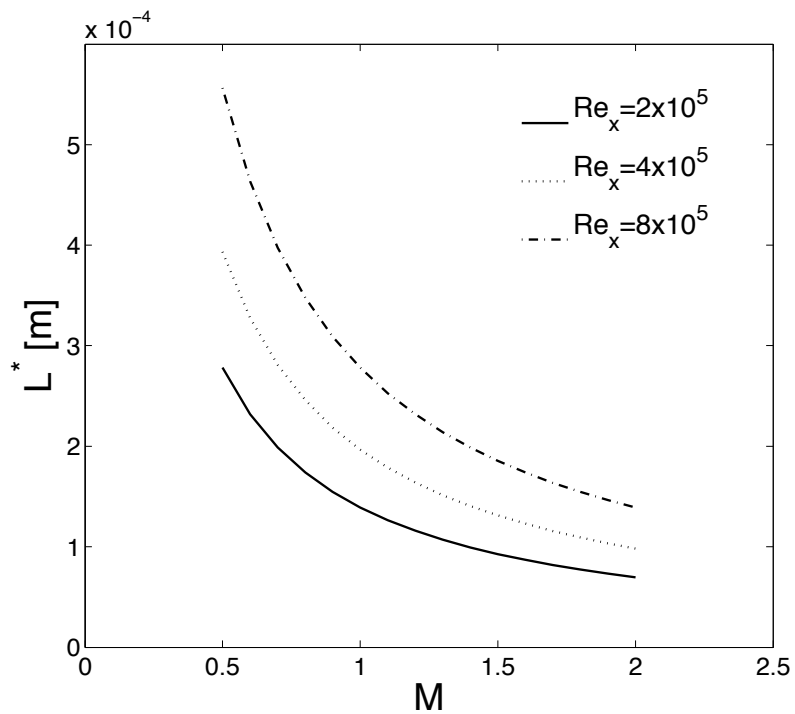
$M_\infty=2.0, \text{Re}_x=400k, \omega^*=9f$ DBD



Lengthscales



- Note decrease of L^* and x_d with M_∞ and decreasing Re_x

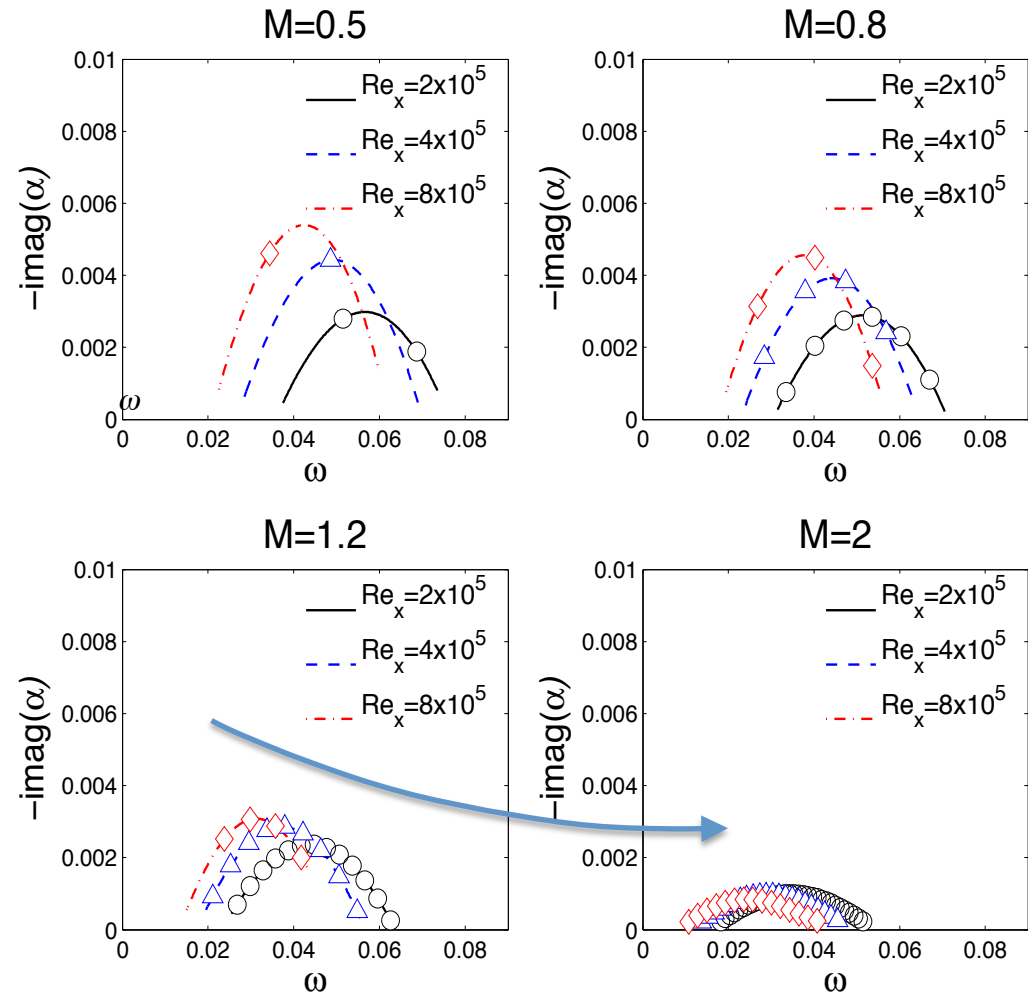




FFT Frequency spectrum

- More modes participate with increasing M_∞ (see symbols)
- Including larger multiples of ω_{DBD} (i.e., with smaller integrated source)

$$\omega = \omega^* \frac{L^*}{u_\infty^*}$$



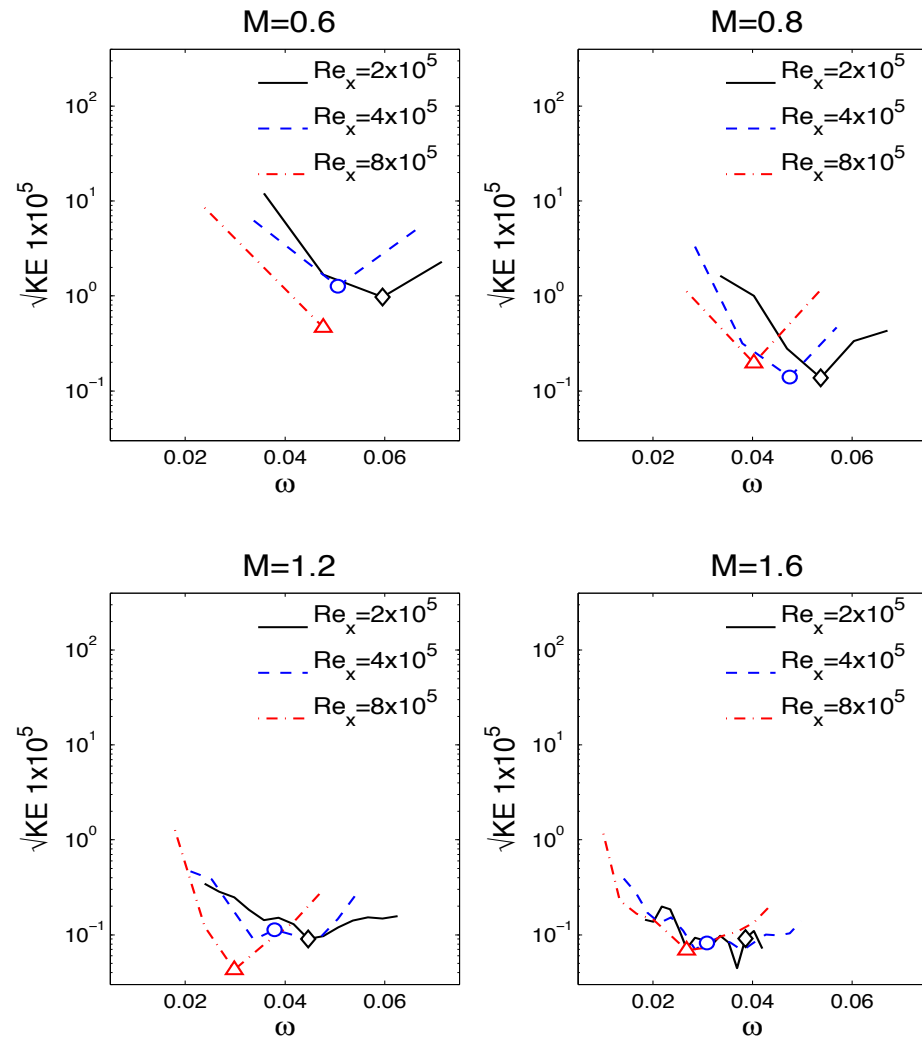


Modal Kinetic Energy

- Kinetic energy independent of mode k normalization

$$KE_k = |A_k|^2 \int_0^\infty \rho \hat{\phi}_k^\dagger(y) \phi_k(y) dy$$

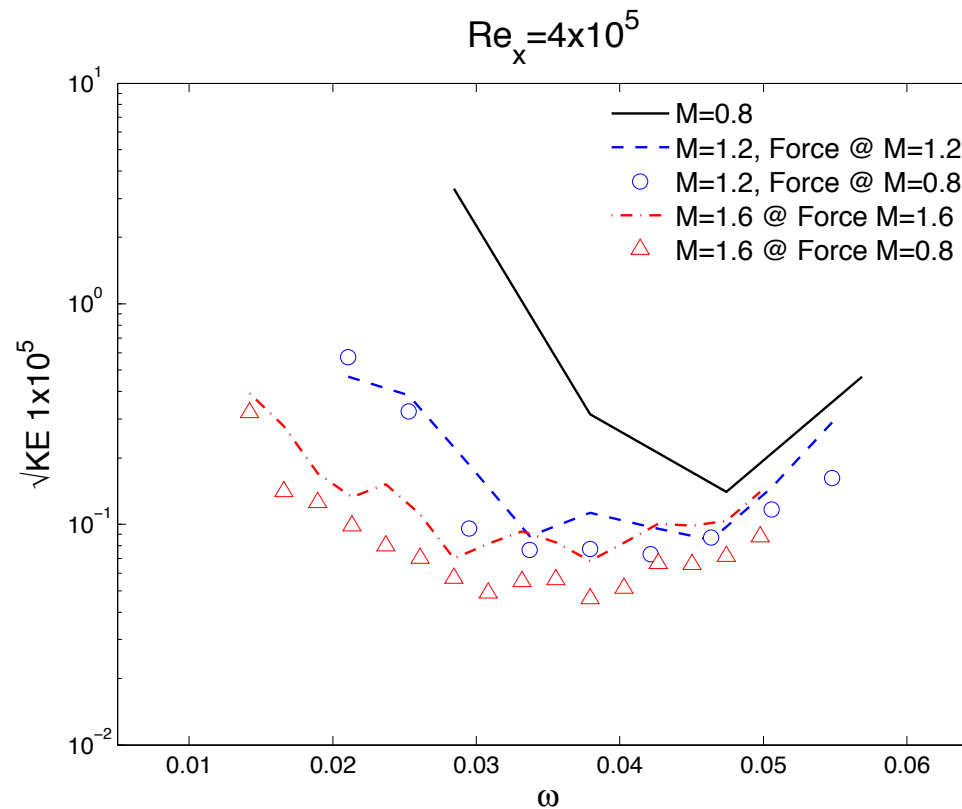
- Symbols show the most amplified mode $\max(\text{Im}(-\alpha))$
- Non-monotoneous response to Re_x . Decreased effect at $M_\infty=1.6$





Effect of Force

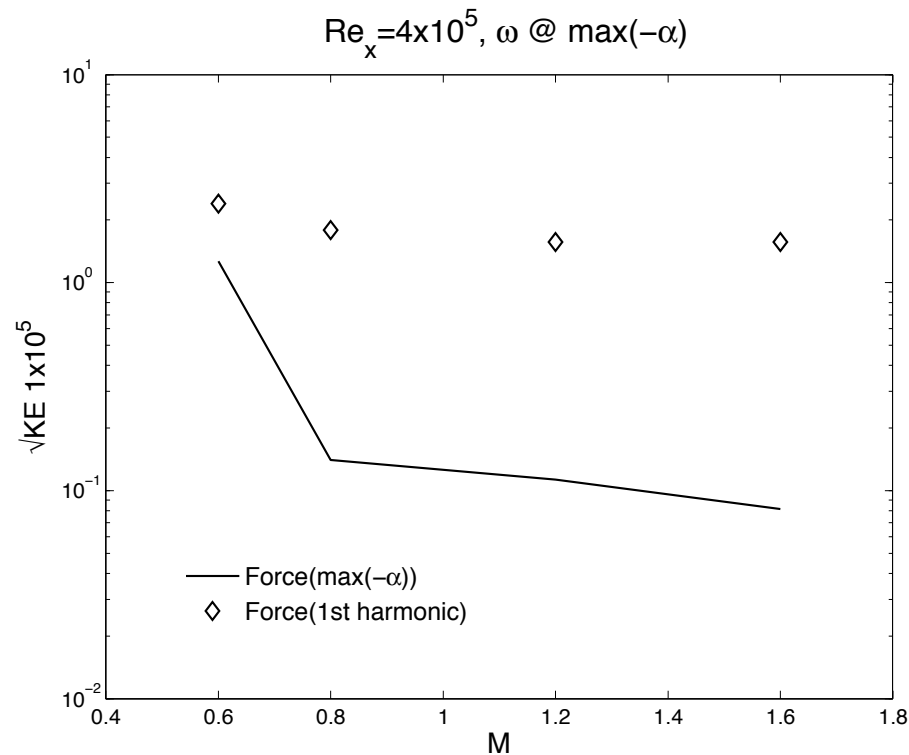
- Using the force FFT components at $M_\infty=0.8$ for $M_\infty=1.2, 1.6$
- Relatively insensitive receptivity response to M -variation, as expected from the slight force profile change observed on slide #26





Force Mode Shape Effect

- Using 1st harmonic mode (symbols) instead of actual harmonic @ $\max(\text{Im}(-\alpha))$
- Suggests benefit in selecting DBD frequency at the most amplified mode
- Possible trade-off as DBD thrust diminishes with frequency



Outline



- Introduction
- Linear Stability Analysis Framework
- AMR Coupled Plasma-Navier and Stokes Solver
- Discharge Features
- Receptivity Analysis and Design Implications
- **Summary**

Summary



- An analysis of compressible effects on flow receptivity to DBD actuation in a 2D set up with He gas was presented.
- The dependence of the force, peak velocity and integrated source term on flow conditions was investigated.
- The main findings in terms of receptivity can be summarized as follows
 - Receptivity decreases between $M_\infty=0.5-2$, with saturating Re_x effect
 - For an an increase in M , an actuator shift upstream is beneficial to increase the overlap with the highly receptive region
 - For the gas system under consideration, the flow dependence of the force has little effect on receptivity.
 - DBD frequency matching to the most amplified mode may increase receptivity in a frequency range where the force does not degrade much
- A new coupled plasma – Navier and Stokes solver was developed.
- The AMR feature allows for dynamic tracking of the discharge into the volume of the flow, while the embedded boundary capability allows simulating complex 3D geometries.



Future Research

- Reduced air chemistry, with most relevant species/reactions may lead to different conclusion on flow-plasma interactions
- Accelerated numerical models addressing the stiffness of fast chemical reactions
- 3D cross-flow linear, non-linear receptivity and transition studies with plasma roughness elements.

Acknowledgements



- Donald A. Durston and Cetin C. Kiris
- Esteban Cisneros, Grad. Student in Aerospace Engineering at the University of Texas at Arlington, TX
- TACC (Texas Advanced Computing Center) at UT Austin

This presentation includes material from the following publications:
AIAA 2014-0485, AIAA 2012-2737

THANKS

